Transcriptional changes in kidney allografts with histology of antibody-mediated rejection without anti-HLA donor-specific antibodies

Jasper Callemeyn[1,2], Evelyne Lerut[3], Henriette de Loor[1], Ingrid Arijs[4], Olivier Thaunat[5,6,7], Alice Koenig[5,6,7], Vannary Meas-Yedid[8], Jean-Christophe Olivo-Marin[8], Philip Halloran[9], Jessica Chang[9], Lieven Thorrez[10], Dirk Kuypers[1,2], Ben Sprangers[2,11], Leentje Van Lommel[12], Frans Schuit[12], Marie Essig[13], Wilfried Gwinner[14], Dany Anglicheau[15,16,17], Pierre Marquet[18], Maarten Naesens[1,2,†]

[1] Nephrology and Renal Transplantation Research Group, Department of Microbiology, Immunology and Transplantation, KU Leuven, Leuven, Belgium

[2] Department of Nephrology and Renal Transplantation, University Hospitals Leuven, Leuven, Belgium

[3] Department of Morphology and Molecular Pathology, University Hospitals Leuven, Leuven, Belgium

[4] Laboratory for Translational Genetics, Department of Human Genetics, KU Leuven, VIB Center for Cancer Biology, Leuven, Belgium

[5] CIRI, INSERM U1111, Université Claude Bernard Lyon I, CNRS UMR5308, Ecole Normale Supérieure de Lyon, Univ. Lyon, 21, avenue Tony Garnier, 69007 Lyon, France

[6] Université Claude Bernard Lyon I; Lyon, France

[7] Department of Transplantation, Nephrology and Clinical Immunology, Edouard Herriot Hospital, Hospices Civils de Lyon, Lyon, France.

[8] Unité d'Analyse d'Images Biologiques, Institut Pasteur, CNRS URA 2582, Paris, France

[9] Department of Medicine, Division of Nephrology and Transplant Immunology, University of Alberta, Edmonton, Canada

[10] Department of Development and Regeneration, KU Leuven, Leuven, Belgium

[11] Department of Microbiology and Immunology, Laboratory of Molecular Immunology, Rega Institute, KU Leuven, Leuven, Belgium

[12] Gene Expression Unit, Department of Cellular and Molecular Medicine, KU Leuven, Leuven, Belgium

[13] CHU Limoges, Department of Nephrology, Dialysis and Transplantation, University of Limoges, Limoges, France

[14] Nephrology, Internal Medicine, Hannover Medical School, Hannover, Germany

[15] Paris Descartes, Sorbonne Paris Cité University, Paris, France

[16] INSERM U1151, Paris, France

[17] Department of Nephrology and Kidney Transplantation, Necker Hospital, Assistance Publique-Hôpitaux de Paris, Paris, France

[18] INSERM U1248, Limoges, France; CHU Limoges, France; Université de Limoges, Limoges, France

† **Corresponding author**

Maarten Naesens, MD, PhD

ORCID ID https://orcid.org/0000-0002-5625-0792

Department of Nephrology and Renal Transplantation, University Hospitals Leuven

Herestraat 49, 3000 Leuven, Belgium

Tel: +32 16 34 45 80; Fax: +32 16 34 45 99

Email: maarten.naesens@uzleuven.be

Running title: Transcriptomics of ABMR histology

Abstract word count: 249; **Text word count: 3783**

Keywords

Antibody-mediated rejection, kidney transplantation, transcriptomics, donor-specific antibodies, natural killer cells

Significance statement

Donor-specific anti-HLA antibodies (HLA-DSA) are often not present in serum of patients with histology of antibody-mediated kidney allograft rejection (ABMR). This causes doubt in clinical decision-making. This study shows that ABMR histology associates with a distinct transcriptional profile, independent of the presence of HLA-DSA. Molecular assessment of allograft biopsies does not allow elucidating the underlying cause of ABMR histology, although HLA-DSA are an independent risk factor for graft failure after ABMR histology. The important heterogeneity in the underlying stimuli and related outcome of ABMR histology, despite the homogeneous histomolecular phenotype, indicates that therapeutic decisions should not be based solely on the histological and molecular presentation. All efforts should go to identifying and targeting the underlying stimulus of ABMR histology.

Abstract

Background: Circulating anti-HLA donor-specific antibodies (HLA-DSA) are often absent in serum of kidney allograft recipients with biopsies demonstrating histology of antibody-mediated rejection (ABMRh). It is unclear whether HLA-DSA negative ABMRh represents a distinct clinical and molecular phenotype.

Methods: In this BIOMARGIN multicenter cohort study, we integrated allograft microarray analysis with extensive clinical and histological phenotyping from 224 kidney transplant recipients between 2011 and 2017. ABMRh was termed for biopsies fulfilling the first two Banff 2017 criteria for antibody-mediated rejection, irrespective of HLA-DSA status.

Results: ABMRh was present in 56/224 biopsies, in 26/56 cases (46.4%) without detectable serum HLA-DSA. ABMRh biopsies showed overexpression of transcripts mostly related to IFNγ-induced pathways, natural killer cell activation and endothelial cell activation. Pathways were upregulated to a similar extent in both HLA-DSA positive and HLA-DSA negative cases of ABMRh, with similar enrichment of infiltrating leukocytes. Transcriptional heterogeneity within ABMRh was caused by concomitant T-cell mediated rejection, but not by HLA-DSA status. Despite the absence of transcriptional differences, HLA-DSA positive ABMRh associated with a higher risk of graft failure than HLA-DSA negative ABMRh in comparison to cases without ABMRh (HR 7.24, 95% CI 3.04-17.20 and HR 2.33, 95% CI 0.85-6.33, respectively).

Conclusion: ABMR histology corresponds to a robust intragraft transcriptional signature, irrespective of the HLA-DSA status. Outcome after ABMR histology is not solely determined by the histomolecular phenotype but is predicted by the underlying etiological factor. It is important to consider this heterogeneity in further research and in treatment decisions in patients with ABMR histology.

Introduction

Although short term outcome after kidney transplantation has significantly improved in the past decades, long term allograft survival has not increased to a similar extent.[1,2] Currently available immunosuppressive agents are able to prevent and treat T cell-mediated rejection (TCMR), but are less potent for antibody-mediated rejection (ABMR), which has now become a prominent cause of late graft failure.[3–6]

Historically, the Banff consortium defined ABMR based on histologic criteria combined with serologic evidence of donor-specific HLA antibodies (HLA-DSA).[7] However, despite increasing sensitivity of antibody detection assays, a significant proportion of patients with the exact same histological picture of ABMR (hereafter referred to as ABMRh), do not have detectable circulating HLA-DSA.[8,9]

In the 2017 Banff revision, C4d deposition in peritubular capillaries, circulating non-HLA antibodies, and intrarenal ABMR-associated transcripts were added as surrogate third criteria.[10] However, further validation of this adaptation is warranted. First, although C4d deposition is associated with HLA-DSA, we recently showed that C4d deposition does not associate with outcome in cases with HLA-DSA negative ABMRh, which was similar to outcome of a control group without ABMRh.[8,11,12] Second, non-HLA antibodies constitute a broad range of autoantibodies with high inter-patient variability, and assessment of non-HLA antibodies is complicated by uncertainty about mean fluorescence intensity cut-off values.[13–15] Third, currently reported molecular classifiers are based on ABMR-associated transcripts, but validation on different sequencing platforms and in independent cohorts is lacking. Finally, recent evidence indicates that microvascular inflammation on graft biopsy is not always triggered by antibody, but instead sometimes results from direct NK cell activation by missing self, suggesting the possibility of alternative explanations.[16]

In this multicenter study, we aimed to elucidate whether the transcriptional profile of biopsies with HLA-DSA negative ABMRh can indicate an undetected humoral etiology, or whether HLA-DSA negative ABMRh should be considered as a distinct histomolecular entity. For this purpose, we investigated the transcriptome of 224 prospectively collected kidney allograft biopsies.

Methods

Population and data collection

224 renal allograft biopsy samples from 224 single kidney allograft recipients were collected in four European transplant centers between June 2011 and March 2017 (University Hospitals Leuven, Belgium; Medizinische Hochschule Hannover, Germany; Centre Hospitalier Universitaire Limoges, France; and Hôpital Necker Paris, France), in the context of the BIOMArkers of renal Graft INjuries (BIOMARGIN) study (www.biomargin.eu; ClinicalTrials.gov number NCT02832661), and the Reclassification using OmiCs integration in KidnEy Transplantation (ROCKET) study. All transplantations were performed with negative complement-dependent cytotoxicity crossmatches. In these four clinical centers, protocol biopsies were performed at 3, 12, and sometimes at 24 months after transplantation, according to local center practice, in addition to the indication biopsies. Institutional review boards and national regulatory agencies (when required) approved the study protocol at each clinical center. Each patient contributed one biopsy. Independent validation was performed on data of computer-assisted analysis of graft inflammation (CAGI) in 47 biopsies collected at Edouard Herriot Hospital and Jules Courmont Hospital (Lyon, France), as recently reported by Sicard et al.[17] The microarray gene expression data from an independent cohort originally described by Sellarés et al., publicly available in the Gene Expression Omnibus of the National Institutes of Health (http://www.ncbi.nlm.nih.gov/geo/)(GSE36059), were used as second independent validation set.[18]

Clinicopathological assessment

Histological lesions were scored according to the Banff 2017 criteria by a local expert pathologist in each participating center.[10] The term "ABMRh" was used for biopsies that fulfilled the first two (histological) Banff criteria for ABMR, by the combination of Banff scores for glomerulitis, peritubular capillaritis, arteritis, thrombotic microangiopathy and C4d deposition. As per Banff 2017 guidelines, glomerulonephritis was considered as an exclusion criterion for ABMRh, as well as peritubular capillaritis without glomerulitis in the presence of borderline rejection, TCMR or polyoma-associated nephropathy. For diagnosis of borderline rejection, the threshold of $i > 0$ in the presence of $t > 0$ was used. HLA-DSA after transplantation were determined per local center practice. HLA-DSA positivity was defined as detectable donor-specific serum anti-HLA antibodies with a mean fluorescence intensity

value of more than 500 at the moment of biopsy or any time before. In order to delineate a strict definition of HLA-DSA negative ABMRh, patients with resolved HLA-DSA at time of the biopsy, but with previously detectable HLA-DSA, were allocated to the HLA-DSA positive group. In the external microarray cohort from Edmonton (GSE36059), biopsies determined as mixed rejection, ABMR or possible ABMR in the original study were considered as ABMRh. Data on patient HLA-DSA status were not available in the public dataset but provided to us by the corresponding author. For the external computerized imaging data, details were published previously.[16,17] Briefly, double stainings with anti-CD34 (endothelial cells) and respectively one antibody among anti-CD3 (T cells), anti-CD20 (B cells), anti-CD66b (granulocytes), anti-CD68 (macrophages) and anti-CD56 (NK cells) were performed by immunochemistry on paraffin-embedded sections using an anti-human CD34 (clone QBEnd10, 1/200, Dako, Les Ulis, France) and respectively anti-human CD3 (clone SK7, 1/150, Becton Dickinson, Le Pont de Claix, France), anti-human CD20 (Clone L26, 1/400, Dako), anti CD66b (clone G10F5, 1/300,Becton Dickinson), anti-human CD68 (clone PGM1, 1/100, Dako) and anti-human CD56 (clone CD564, 1/10, produced by Novocastra and distributed by Leica Microsystemes SAS, Nanterre, France). Computerized quantitative analyses were conducted to quantify the density of each immune cell type in the microcirculation and tubulointerstitial compartment of the renal allograft.[17]

Biopsy sample collection and transcriptomic analysis

Two needle cores were taken at each kidney allograft biopsy. One was used for histology, at least half of the other was immediately stored in Allprotect Tissue Reagent® (Qiagen, Benelux BV, Venlo, The Netherlands). The Allprotect tubes were stored at 4°C (min 24 hours - max 72 hours), and then stored at -20°C until RNA extraction. Total RNA was isolated from the kidney allograft biopsy specimens - using the Allprep DNA/RNA/miRNA Universal Kit® (Qiagen Benelux BV) on a QIAcube instrument (Qiagen Benelux BV). The quantity (absorbance at 260nm) and purity (ratio of the absorbance at 230, 260 and 280nm) of the isolated RNA were measured using the NanoDrop ND-1000™ spectrophotometer (Thermo Scientific™, Life Technologies Europe BV, Ghent, Belgium). RNA integrity was evaluated with the Eukaryote nano/pico RNA Kit® (Agilent Technologies Belgium NV, Diegem, Belgium) on the Bioanalyzer 2100 instrument™ (Agilent Technologies Belgium NV). The

extracted RNA was subsequently stored at -80°C until microarray analysis. The arrays were washed and stained with streptavidin-phycoerytrin on an automated Fluidics Station (Affymetrix) and scanned on the GeneChip® Scanner 3000 7G System (Affymetrix). Total RNA extracted from the biopsy samples was first amplified and biotinylated to complementary RNA (cRNA) using the GeneChip® 3' IVT PLUS Reagent Kit (Affymetrix Inc., High Wycombe HP10 0HH, UK). The quality of labelled and fragmented cRNA was assessed with the Agilent 2100 Bioanalyzer. Fragmented cRNA was hybridized to the Affymetrix GeneChip Human Genome U133 Plus 2.0 Arrays (Affymetrix), which comprised of 54,675 probe sets covering the whole genome. The arrays were washed and stained with streptavidin-phycoerytrin on an automated Fluidics Station (Affymetrix) and scanned on the GeneChip® Scanner 3000 7G System (Affymetrix). The resulting image files (.dat files) were generated using the GeneChip® Command Console® Software (AGCC), and intensity values for each probe cell (.cel file) were calculated. The microarray data were handled accordance with the MIAME (Minimum Information About a Microarray Experiment) guidelines. The microarray gene expression data is available at the Gene Expression Omnibus database under the accession number GSE147089.

Data analysis

The microarray data were analysed using TAC software (version 4.0, Thermo Fisher Scientific, Carlsbad, CA, United States) and Bioconductor tools in R (v3.5.3,www.rstudio.com).[19] The robust multichip average method was performed on the raw expression data (.cel files) to obtain a log2 expression value for each probe set, and batch effect correction was performed for timing of the microarray analysis by use of the LIMMA package.[20,21] For comparative analysis, the LIMMA package was used to identify the gene probe sets that showed significant differential expression between the studied groups, based on moderated t-statistics with Benjamini-Hochberg false discovery rate (FDR) correction for multiple testing.[21] FDR-adjusted P-values less than 0.01 were considered significant. The Bio Functional Analysis tool in the Ingenuity Pathway Analysis program (IPA; Ingenuity Systems®) was used to identify the biological functions associated with the datasets of significantly differentially expressed gene probe sets. Deconvolution analysis was performed by the online CIBERSORT tool (https://cibersort.stanford.edu/).[22] Briefly, by application of the LM22 gene signature matrix, the relative

infiltration pattern of 11 major leukocyte types, corresponding to 22 leukocyte subtypes, within each biopsy was calculated. To estimate absolute infiltration within a specific biopsy, calculated relative leukocyte fractions were multiplied by the ratio of *CD45* expression within the biopsy, a pan-leukocyte marker, to the mean *CD45* expression in a group of normal biopsies, resulting in a dimensionless parameter.[23] Dimensionality reduction of expression data was performed using t-distributed stochastic neighbour embedding (t-SNE).[24] A weighted gene co-expression network analysis (WGCNA) was performed in order to correlate clinical traits with transcriptional heterogeneity within biopsies.[25] In order to construct a topological overlap matrix, co-expression similarity was defined by biweight midcorrelation with a soft threshold power value of 13, corresponding to a scale-free topology fitting index of 0.886. Co-expressing gene probe sets were assigned to modules by average linkage hierarchical clustering, with a minimal module size set at 30 gene probe sets with a deepSplit=3. Modules were merged if similarity was > 0.75. Module-trait association testing was performed with the application of a false discovery rate (FDR) correction with a cut-off of 0.05.

For clinicopathological features, nominal variables were compared utilizing Chi-Square test, or Fisher's exact test where appropriate. Comparison of continuous variables was performed by T test/ANOVA or Mann-Whittney U/Kruskal-Wallis test procedure for normal and non-normal distributed data, respectively. Two-sided hypothesis tests with a significance level of less than 0.05 were considered significant. For the computerized imaging data, principal component analysis with 95% confidence ellipses were used to integrate leukocyte subtype quantities within different renal compartments. We used SAS (version 9.4, SAS Institute Inc., Cary, NC, United States) for statistical analysis and GraphPad Prism (version 8.0.1, GraphPad Software, San Diego, CA, United States) for graphical presentation.

Results

Study population, demographics and histology

Of the 224 included kidney allograft biopsies, ABMRh was identified in 56 cases. Of these, 30/56 cases (53.6%) had concomitant or previous documentation of HLA-DSA (HLA-DSA positive ABMRh). Importantly, in 11/30 cases (36.7%), HLA-DSA had resolved at the time of biopsy. Conversely, in 26/56 ABMRh cases (46.4%), no anti-HLA donor specific antibodies were or had ever been detected (HLA-DSA negative ABMRh). In this group, 8/26 (30.8%) biopsies showed C4d deposition, thus fulfilling the Banff 2017 criteria for active ABMR.[10]

Compared to other cases, ABMRh cases were identified more often at indication than at protocol biopsies, with higher proteinuria and lower eGFR at time of the biopsies (**Table 1**). In addition, delayed graft function had preceded ABMRh biopsies more frequently (34.6% vs. 17.4%), and more specifically associated with HLA-DSA negative than HLA-DSA positive ABMRh (46.2% vs. 24.1%), although this trend did not reach statistical significance, P=0.09). Patients with HLA-DSA positive ABMRh had received a kidney transplant at a younger age than patients with HLA-DSA negative ABMRh (43.3 vs. 52.5 years, P=0.02). Other recipient and donor characteristics were similar between groups. Treatment of ABMRh occurred more often after indication than protocol biopsies (29/36 vs. 7/20, P<0.001), without differences between HLA-DSA groups, although HLA-DSA positive patients received intravenous immunoglobulins more often.

Apart from the defining histological lesions, ABMRh biopsies also had more tubulitis and interstitial inflammation, with TCMR diagnosed in 14/56 (25.0%) vs. 10/168 (6.0%) biopsies without ABMRh (P<0.001). Except for more C4d deposition in ABMRh biopsies with HLA-DSA, there were no histological differences between HLA-DSA positive ABMRh and HLA-DSA negative ABMRh (**Table 2)**.

Transcriptional comparison of HLA-DSA positive and HLA-DSA negative ABMRh subtypes

Next, whole transcriptome analysis of all 224 biopsies was performed. In comparison to other biopsies, we identified upregulation of 3848 transcripts in ABMRh biopsies, corresponding to 1756 genes, and

downregulation of 2516 transcripts, or 1436 genes (**Figure 1A, Table S1**). Among the differentially expressed gene list were 19/23 previously reported DSA specific transcripts (DSASTs) and 16/20 ABMR classifiers, reflecting a high similarity to previously reported ABMR cohorts.[18,26] Comparing HLA-DSA positive ABMRh and HLA-DSA negative ABMRh, only sex-specific genes were expressed with a more than 2-fold change, reflecting a higher tendency of female donors in the HLA-DSA positive group (64.3% vs. 48.0% female donors, respectively). After correction for multiple testing, no transcripts were differentially expressed between HLA-DSA positive and HLA-DSA negative cases (**Figure 1B**). Alternative stratification of ABMRh biopsies using C4d positivity, HLA-DSA status at time of the biopsy, the third Banff 2017 criterion (C4d- or DSA-positive) and concomitant borderline changes or TCMR did not reveal transcriptional differences between groups either (**Figure S1**). Similarly, if microvascular inflammation (MVI, defined as g+ptc score ≥2) was used, no differences were observed between HLA-DSA positive and HLA-DSA negative MVI cases. To corroborate these findings, we analyzed gene expression data from an external cohort,[18] and again found no differentially expressed genes between HLA-DSA negative ABMRh (n=10) and HLA-DSA positive ABMRh (n=87) cases (**Figure S2)**.

Pathway analysis revealed an upregulation of 269 distinct genetic pathways in ABMRh vs. biopsies without ABMRh. The most significantly enriched pathways were related to T helper cell activation and maturation, antigen presentation, natural killer (NK) cell signalling, crosstalk between dendritic cells and NK cells, and crosstalk between the innate and adaptive immune system (**Table S2).**[23] These pathways were similarly enriched when HLA-DSA negative ABMRh and HLA-DSA positive ABMRh were compared separately to biopsies without ABMRh (**Figure 1C**).

Leukocyte infiltration and histology of ABMR

Next, we studied the association between leukocyte infiltration and histological findings. Considering that many probe sets are not specific for immune cell subsets, we used CIBERSORT deconvolution analysis based on the LM22 gene signature matrix to estimate intragraft leukocyte infiltration.[22] Leukocyte infiltration correlated better with acute than chronic histological lesions. Irrespective of patient HLA-DSA status, NK cells and monocytes/macrophages most strongly associated with severity

of glomerulitis, peritubular capillaritis and vasculitis, and less with C4d deposition or transplant glomerulopathy (**Fig 2A, Fig S3)**. The infiltration of other leukocyte subtypes also correlated with severity of microvascular inflammation, with the exception of γδ T cells, which associated mostly with TCMR lesions, neutrophils and eosinophils.

In HLA-DSA negative patients, NK cell infiltration had the highest diagnostic accuracy for ABMRh (AUC=0.87), followed by monocytes/macrophages (AUC=0.84) and CD8 T cells (AUC=0.82) (**Fig 2B-C, Table S3)**. Similarly in HLA-DSA positive patients, ABMRh was best predicted by monocytes/macrophages (AUC=0.87), NK cells (AUC=0.84) and CD8 T cells (AUC=0.83). However, no leukocyte subtypes could differentiate HLA-DSA positive from HLA-DSA negative ABMRh.

To validate our finding that leukocyte infiltration did not differ between phenotypes of ABMR histology, we analyzed 47 independent biopsies with MVI using the Computer-assisted Analysis of Graft Inflammation (CAGI) technique, which allows the quantification of macrophages, T cells, B cells, and granulocytes per unit surface of interstitium and microcirculation. In line with our findings using CIBERSORT deconvolution, T cells and macrophages constituted the most abundant cell types in MVI biopsies, whereas NK cells formed a minority of infiltrating cells. A comparison between HLA-DSA positive MVI (n=32) and HLA-DSA negative MVI (n=15) did not show any differences in leukocyte subset infiltration, both within the interstitial and microcirculatory compartment (**Figure S4**). Principal component analysis of the entire dataset showed a major overlap between groups, suggesting that similar cellular infiltrates account for MVI lesions in both HLA-DSA positive and HLA-DSA negative patients (**Figure 3**).

Molecular heterogeneity of ABMRh

Given the absence of molecular differences between HLA-DSA positive ABMRh and HLA-DSA negative ABMRh, we next investigated whether the ABMRh biopsy cohort was homogeneous at the transcriptional level. Based on expression data from all probe sets, t-SNE was used to visualize distance between biopsies **(Fig 4A**). In addition, t-SNE was also performed using subsets of probe sets representing genes associated with NK cells[22], antibody-dependent cellular cytotoxicity (ADCC)[27] and

antibody-mediated rejection – including DSASTs.[28] Selective gene subsets discriminated most ABMRh cases from cases without ABMRh, whereas biopsies with HLA-DSA positive ABMRh co-clustered with the HLA-DSA negative ABMRh cases (**Fig 4B-D**).

However, 10 ABMRh biopsies were persistent outliers, regardless of the applied gene list. In general, these outlier biopsies had less MVI, less additional tubulointerstitial inflammation, and more IFTA than the other ABMRh biopsies, although timing and allograft function were similar (**Table S4)**. Interestingly, in the outlier group, CIBERSORT-estimated leukocyte infiltration was similar to cases without ABMRh (**Figure S5**).

Next, focusing solely on ABMRh biopsies, molecular heterogeneity was revealed, which could be partially attributed to clustering of biopsies with mixed rejection (**Figure 4E-H**). Neither HLA-DSA status nor biopsy C4d deposition could account for the molecular heterogeneity within ABMRh biopsies.

We evaluated whether ABMR specific transcripts correlated with the histomorphological ABMR lesion scores in different HLA-DSA conditions, by grouping the samples according to serum HLA-DSA status and calculation of the sum of glomerulitis, peritubular capillaritis, C4d deposition, arteritis and transplant glomerulopathy. Selective gene sets co-localized biopsies with similar humoral lesion scores regardless of HLA-DSA status, demonstrating that similar genes are associated with ABMR lesion severity in HLA-DSA negative patients (**Figure 5**).

To further investigate the transcriptional heterogeneity within ABMRh, WGCNA was performed to identify modules of co-varying genes. Within ABMRh biopsies, 37 modules were identified, of which none significantly associated with HLA-DSA status (**Figure 6**). Borderline rejection or C4d score did not correlate with expressional variation within ABMRh cases either. In contrast, module-trait analysis associated 5 modules with concomitant TCMR. These findings confirm that the transcriptional variability seen in ABMRh biopsies is not caused by HLA-DSA status, but rather reflects the presence of concomitant TCMR.

Graft survival after ABMRh diagnosis

We next assessed whether our findings, that HLA-DSA status did not influence the molecular picture of ABMRh, were also reflected by similarity in graft outcome between HLA-DSA positive and negative cases (**Figure 7)**. In a univariate Cox proportional hazards analysis, HLA-DSA positive ABMRh associated with a higher risk of graft failure than HLA-DSA negative ABMRh (HR 5.39, 95% CI 2.55-11.34 and HR 2.57, 95% CI 1.00-6.58, respectively), together with TCMR, whereas C4d score and borderline rejection did not (**Table 3**). De novo HLA-DSA conferred a higher risk of allograft failure than pretransplant HLA-DSA, compared to cases without HLA-DSA (HR 5.60, 95% CI 2.49-12.6 and HR 2.48, 95% CI 1.10-5.59, respectively). At the time of biopsy, both persisting and resolved HLA-DSA were positively associated with graft failure (HR 3.75, 95% CI 1.68-8.39 and 3.93, 95% CI 1.67-9.21, respectively). . In a multivariate analysis, only HLA-DSA positive ABMRh remained significant (HR 7.24, 95% CI 3.04-17.20), whereas HLA-DSA negative ABMRh lost effect on graft outcome (HR 2.33, 95% CI 0.85-6.33). In a multivariate analysis of ABMRh, HLA-DSA, biopsy timing, total cortical inflammation and chronic lesions, we found that ABMRh and HLA-DSA remained independent predictors of failure, along with ti, IFTA grade and cg (**Table S5).**

A molecular score based on the mean expression of NK cell, ADCC or ABMR associated transcripts univariately associated with graft outcome (**Figure 7D-E)**. ABMRh lost its prognostic significance when combined with molecular scores for ADCC and ABMR in a multivariate model (**Table S6**).

Discussion

Donor-specific antibodies are considered pivotal in the pathogenesis of microvascular inflammation of kidney allografts, but often remain undetectable in serum of patients with the histology of antibody-mediated rejection. In this study, we demonstrated that there are major transcriptomic alterations in biopsies with ABMRh, involving pathways related to NK cell activation, crosstalk between innate and adaptive immunity, T helper cell activation and IFN-γ signalling cascades. ABMRh was related to a specific immune cell infiltrate, hallmarked mainly by NK cells, monocytes/macrophages and CD8+ T cells. The transcriptional picture of ABMRh was highly similar to the molecular landscapes that have been published by others in association with ABMR, which supports the robustness and relevance of ABMRh as a distinct phenotype.[18,29,30] Taking into account patient HLA-DSA status, there were no transcriptomic differences between cases with and without detectable HLA-DSA. In addition, no leukocyte subtype, estimated by CIBERSORT, could differentiate between HLA-DSA positive and HLA-DSA negative ABMRh groups. Although the accuracy of the CIBERSORT algorithm for intrarenal immune cell infiltration has not been validated yet, this was confirmed in an independent cohort with leukocyte subset infiltration quantified using computerized analysis of immunohistochemical staining. Despite the similar histomolecular characteristics and treatment numbers after diagnosis, the outcome of HLA-DSA positive ABMRh was significantly worse than HLA-DSA negative ABMRh. This suggests that the outcome of ABMRh is determined rather by its underlying cause than by its histomolecular presentation.

The strength of this study lies in the deep integration of transcriptomics with extensive histological and serological phenotyping. To our knowledge, this is the first molecular analysis of ABMRh that studies the effect of HLA-DSA status on the biopsy transcriptome. Importantly, our findings were confirmed in the GSE36059 dataset described by the Edmonton group, where HLA-DSA negative ABMRh had a similar transcriptional picture as HLA-DSA positive ABMRh.[18]

The histomolecular similarity in of ABMRh biopsies with and without HLA-DSA could be explained by common pathophysiology. It is plausible that enrichment of similar genes in HLA-DSA negative ABMRh biopsies implies the involvement of undetected humoral aetiology. Indeed, ADCC-associated

genes correlate with severity of humoral lesions also in HLA-DSA negative patients. The immunogenicity of genetic mismatches at non-HLA loci was supported by the higher incidence of non-HLA antibodies in mismatched patients.[31,32] Moreover, non-HLA antibodies have been related to endothelial cell activation, microvascular inflammation and graft survival.[13,14,33] Alternatively, HLA-DSA may remain undetected in serum in case of intragraft absorption or antibody production within intragraft tertiary lymphoid aggregates.[34,35] In addition, the indirect pathway of allorecognition, pivotal for B cell differentiation into antibody-producing plasma cells, allows for generation of memory B cells, capable of an enhanced immune response upon secondary antigen presentation even when HLA-DSA have disappeared from the circulation.[9,36–39] Nevertheless, in this study, circulating donor-specific anti-HLA antibodies associated with worse allograft survival, confirming previously reported findings.[8] It could be that donor-specific non-HLA antibodies, non-circulating anti-HLA antibodies or memory B cells are less pathogenic than circulating anti-HLA antibodies and associate with better outcome.

To explain these differences in terms of allograft outcome, we speculate that the temporal dynamics of HLA-DSA negative ABMRh are of relevance. Previously, our research group has shown that HLA-DSA negative ABMRh associates with lower ABMRh recurrence and incidence of transplant glomerulopathy on sequential allograft biopsies than HLA-DSA positive ABMRh.[8] The more time-constrained nature of HLA-DSA negative ABMRh appears to cause less subsequent chronic allograft damage, and could therefore promote better outcome. Also in the current study, these chronic lesions conferred worse outcome, concordant with this hypothesis. Future transcriptional studies could investigate this temporal aspect by longitudinal follow-up of ABMRh cases.

The differences between HLA-DSA positive and negative cases in ABMRh recurrence suggest that the underlying stimulus of DSA negative ABMRh is more transient or weaker than detectable HLA-DSA. Aside from undetected humoral causes, the ABMRh phenotype could be induced by other phenomena. NK cells have been demonstrated as essential in the pathogenesis of ABMR, but their activity can also be impacted by non-humoral stimuli.[23,27,40–45] It was recently demonstrated that recipient NK cells, in the absence of donor HLA I-mediated stimulation of their inhibitory killer cell immunoglobulin-like receptors (i.e. “missing self”), can induce endothelial cell damage, leading to chronic vascular rejection

and accelerated graft loss.[16] Although some NK cell transcripts differ based on the underlying stimulus, the transcriptional profile of activated NK cells by induced self, missing self or ADCC shows significant overlap.[46] Therefore, inferring aetiology of NK cell activation from expressional data may not be straightforward. We hypothesize that transient NK cell stimuli can induce similar histomolecular changes as ADCC-induced damage but render less long-term harm to the allograft given their time-constrained nature. Indeed, delayed graft function after transplantation is linked with an increased risk of allograft rejection,[47] and tended to precede HLA-DSA negative ABMRh biopsies more often in this cohort.

Our findings are of relevance for classification of allograft biopsies. In the revised 2017 Banff criteria for ABMR, C4d deposition was added to HLA-DSA as an alternative third criterion. However, since neither DSA nor C4d associate with transcriptional heterogeneity within ABMRh, this study does not provide a molecular basis for the third criterion as it is currently defined. Moreover, if C4d is positive in the absence of HLA-DSA, automatic attribution to ABMR might not be appropriate in terms of allograft prognostication given the better outcome. Therefore, it seems important to avoid over-interpretation of causality based on the histological and molecular profiles. In the absence of detectable antibodies, it might be considered to avoid starting aggressive and toxic treatment aiming at reducing antibody levels in the hope to improve outcome. The molecular signals of ABMRh do not seem to help in this aspect of clinical decision-making.

Despite imperfect guidance in therapeutic decisions, our study suggests that molecular assessment of biopsies can contribute to their interpretation. By interrogation of specific gene lists, 10 ABMRh biopsies with a lower molecular score were consistently isolated. These ABMRh outliers had similar HLA-DSA positivity and C4d deposition as other ABMRh biopsies, albeit with less microvascular inflammation, less concomitant tubulointerstitial inflammation and a leukocyte infiltration pattern resembling biopsies without ABMRh. ABMRh is a dichotomous classification, which does not reflect the whole spectrum of lesions present in the biopsies. Using t-SNE informed by expression data for selective gene sets, we identified molecular heterogeneity that goes beyond separation of outliers from the main group, and better reflects the total sum of ABMR lesions. The heterogeneity within ABMRh

was addressed by WGCNA, a data mining method designed to disentangle biological networks, which identified 37 genetic modules. Crucially, only concomitant TCMR associated with specific modules and could thus account for intragroup transcriptional variability, whereas HLA-DSA did not. This further strengthens the finding that HLA-DSA positive and HLA-DSA negative ABMRh cases have a high degree of transcriptional similarity.

This study has several limitations. In order to optimize the definition of HLA-DSA negative ABMRh, we allocated cases with resolved HLA-DSA at the timing of biopsy to the HLA-DSA positive group. A contemporary definition of HLA-DSA status could be more reflective of ongoing processes, although this did not influence results in our sensitivity analysis. We did not assess non-HLA antibodies in our cohort, and we had no information about consecutive allograft histology. Finally, definition of ABMR histology in this study relies on the current Banff 2017 classification.[10] As the diagnostic criteria for rejection after kidney transplantation are a topic of active discussion, our reference standard of histology is imperfect. Relying on MVI as a more direct reflection of the histological lesions without interpretation also did not change our conclusions. Finally, this study represents a selection of biopsies, and does not represent real-life disease prevalence. Although this would not affect our conclusions, including more intermediate cases with incomplete phenotypes or overlapping phenotypes could provide additional insights in the heterogeneity within cases of ABMRh.

In conclusion, we demonstrate that ABMRh corresponds to a distinct transcriptional profile, irrespective of patient HLA-DSA status. Our data suggest that outcome after ABMRh is determined by the underlying stimulus, which is not reflected in the molecular picture. Future studies are warranted to address whether the general transcriptional signature of ABMRh derives from common humoral aetiology or represents a final common pathway that can be initiated by humoral and non-humoral factors. In ABMRh cases, therapeutic decisions should not be based solely on the histological and molecular presentation, but all efforts should go to identifying and targeting the underlying stimulus.

Author contribution

MN, DA, WG, ME and PM designed the study. JC, MN, IA, LT and OT performed data analysis and interpretation. MN, EL, DA, WG, ME, HdL, DK, BS, LVL and FS were involved in data and sample collection for the BIOMARGIN cohort, sample extraction and quality control, and in the microarray experiments. OT, AK, VMY and JCOM collected and analyzed the computerized imaging data. PH and JCh provided data for the external microarray cohort. The manuscript was written by JC and MN, and was revised by all co-authors.

Acknowledgements

We thank the clinical centers of the BIOMARGIN and ROCKET consortium, the clinicians and surgeons, nursing staff, and the patients. The BIOMARGIN study is funded by the Seventh Framework Programme (FP7) of the European Commission, in the HEALTH.2012.1.4-1 theme of "innovative approaches to solid organ transplantation" (grant agreement no. 305499). The ROCKET study is funded by the ERAcoSysMed network (H2020 funding framework; grant reference no. JTC2_29). This study is also funded by a C3 internal grant of the KU Leuven (no. C32/17/049). JC is supported by a PhD Fellowship grant from the Research Foundation Flanders (F.W.O.)(1196119N). MN and BS are senior clinical investigators of The Research Foundation Flanders (F.W.O.)(1844019N and 1842919N).

Disclosures

The authors have no conflict of interest to disclose.

SUPPLEMENTARY MATERIAL

Table of contents

References

1. Coemans M, Süsal C, Döhler B, Anglicheau D, Giral M, Bestard O, et al. Analyses of the short- and long-term graft survival after kidney transplantation in Europe between 1986 and 2015. Kidney Int. 2018;94(5):964–73.

2. Lamb KE, Lodhi S, Meier-Kriesche HU. Long-term renal allograft survival in the United States: A critical reappraisal. Am J Transplant. 2011;11(3):450–62.

3. Halloran PF. Immunosuppressive drugs for kidney transplantation. N Engl J Med. 2004;351(26):2715–29.

4. Pouliquen E, Koenig A, Chen CC, Sicard A, Rabeyrin M, Morelon E, et al. Recent advances in renal transplantation: antibody-mediated rejection takes center stage. F1000Prime Rep. 2015;7(51).

5. Naesens M, Kuypers DRJ, De Vusser K, Evenepoel P, Claes K, Bammens B, et al. The histology of kidney transplant failure. Transplantation. 2014;98(4):427–35.

6. Sellarés J, De Freitas DG, Mengel M, Reeve J, Einecke G, Sis B, et al. Understanding the causes of kidney transplant failure: The dominant role of antibody-mediated rejection and nonadherence. Am J Transplant. 2012;12(2):388–99.

7. Racusen L, Colvin R, Solez K, Mihatsch M, Halloran P, Campbell P, et al. Antibody-mediated rejection criteria - An addition to the Banff ’97 classification of renal allograft rejection. Am J Transplant. 2003;3(6):708–14.

8. Senev A, Coemans M, Lerut E, Van Sandt V, Daniëls L, Kuypers D, et al. Histological picture of antibody-mediated rejection without donor-specific anti-HLA antibodies: Clinical presentation and implications for outcome. Am J Transplant. 2019;19(3):763–80.

9. Luque S, Lúcia M, Melilli E, Lefaucheur C, Crespo M, Loupy A, et al. Value of monitoring circulating donor-reactive memory B cells to characterize antibody-mediated rejection after kidney transplantation. Am J Transplant. 2019;19(2):368–80.

10. Haas M, Loupy A, Lefaucheur C, Roufosse C, Glotz D, Seron D, et al. The Banff 2017 Kidney Meeting Report : Revised diagnostic criteria for chronic active T cell – mediated rejection , antibody- mediated rejection , and prospects for integrative endpoints for next- generation clinical trials. Am J Transplant. 2018;18:293–307.

11. Worthington JE, McEwen A, McWilliam LJ, Picton ML, Martin S. Association between C4d staining in renal transplant biopsies, production of donor-specific HLA antibodies, and graft outcome. Transplantation. 2007;83(4):398–403.

12. Loupy A, Hill GS, Suberbielle C, Charron D, Anglicheau D, Zuber J, et al. Significance of C4d Banff scores in early protocol biopsies of kidney transplant recipients with preformed donor-specific antibodies (DSA). Am J Transplant. 2011;11(1):56–65.

13. Delville M, Lamarthée B, Pagie S, See SB, Rabant M, Burger C, et al. Early acute microvascular kidney transplant rejection in the absence of anti-HLA antibodies is associated with preformed IgG antibodies against diverse glomerular endothelial cell antigens. J Am Soc Nephrol. 2019;30(4):692–709.

14. Dragun D, Müller DN, Bräsen JH, Fritsche L, Nieminen-Kelhä M, Dechend R, et al. Angiotensin II type 1–receptor activating antibodies in renal-allograft rejection. N Engl J Med. 2005;352(6):558–69.

15. Hönger G, Cardinal H, Dieudé M, Buser A, Hösli I, Dragun D, et al. Human pregnancy and generation of anti-angiotensin receptor and anti-perlecan antibodies. Transpl Int. 2014;27(5):467–74.

16. Koenig A, Chen C, Marçais A, Barba T, Mathias V, Sicard A, et al. Missing self triggers NK cell-mediated chronic vascular rejection of solid organ transplants. Nat Commun. 2019;10:5350.

17. Sicard A, Meas-Yedid V, Rabeyrin M, Koenig A, Ducreux S, Dijoud F, et al. Computer-assisted topological analysis of renal allograft inflammation adds to risk evaluation at diagnosis of humoral rejection. Kidney Int. 2017;92(1):214–26.

18. Sellarés J, Reeve J, Loupy A, Mengel M, Sis B, Skene A, et al. Molecular diagnosis of antibody-mediated rejection in human kidney transplants. Am J Transplant. 2013;13(4):971–83.

19. Gentleman RC, and Carey VJ, and Bates DM, and Bolstad B, and Dettling M, and Dudoit S, et al. Bioconductor: open software development for computational biology and bioinformatics. Genome Biol. 2004;5(10):R80.

20. Irizarry R, Hobbs B, Collin F, Beazer-Barclay Y, Antonellis K, Scherf U, et al. Normalization, and summaries of high density oligonucleotide array probe level data. Biostatistics. 2003;4(2):249–64.

21. Ritchie ME, Phipson B, Wu D, Hu Y, Law CW, Shi W, et al. Limma powers differential expression analyses for RNA-sequencing and microarray studies. Nucleic Acids Res. 2015;43(7):e47.

22. Newman AM, Liu CL, Green MR, Gentles AJ, Feng W, Xu Y, et al. Robust enumeration of cell subsets from tissue expression profiles. Nat Methods. 2015;12(5):453–7.

23. Yazdani S, Callemeyn J, Gazut S, Lerut E, de Loor H, Wevers M, et al. Natural killer cell infiltration is discriminative for antibody-mediated rejection and predicts outcome after kidney transplantation. Kidney Int. 2019;95(1):188–98.

24. Laurens van der Maaten, Geoffrey E. H. Visualizing data using t-SNE. J Mach Learn Res. 2008;164(2210):10.

25. Langfelder P, Horvath S. WGCNA: An R package for weighted correlation network analysis. BMC Bioinformatics. 2008;9.

26. Hidalgo LG, Sis B, Sellares J, Campbell PM, Mengel M, Einecke G, et al. NK cell transcripts and NK cells in kidney biopsies from patients with donor-specific antibodies: Evidence for NK cell involvement in antibody-mediated rejection. Am J Transplant. 2010;10(8):1812–22.

27. Parkes MD, Halloran PF, Hidalgo LG. Evidence for CD16a-mediated NK cell stimulation in antibody-mediated kidney transplant rejection. Transplantation. 2017;101:e102–11.

28. Loupy A, Lefaucheur C. Antibody-mediated rejection of solid-organ allografts. N Engl J Med. 2018;379(12):1150–60.

29. Halloran PF, Pereira AB, Chang J, Matas A, Picton M, De Freitas D, et al. Microarray diagnosis of antibody-mediated rejection in kidney transplant biopsies: An international prospective study (INTERCOM). Am J Transplant. 2013;13(11):2865–74.

30. Venner JM, Hidalgo LG, Famulski KS, Chang J, Halloran PF. The molecular landscape of antibody-mediated kidney transplant rejection: Evidence for NK involvement through CD16a Fc receptors. Am J Transplant. 2015;15(5):1336–48.

31. Reindl-schwaighofer R, Heinzel A, Kainz A, Setten J Van, Jelencsics K, Hu K, et al. Contribution of non-HLA incompatibility between donor and recipient to kidney allograft survival: genome-wide analysis in a prospective cohort. Lancet. 2019;6736(18):1–8.

32. Steers NJ, Li Y, Drace Z, D'Addario JA, Fischman C, Liu L, et al. Genomic mismatch at LIMS1 locus and kidney allograft rejection. N Engl J Med. 2019;380(20):1918–28.

33. Lefaucheur C, Viglietti D, Bouatou Y, Philippe A, Pievani D, Aubert O, et al. Non-HLA agonistic anti-angiotensin II type 1 receptor antibodies induce a distinctive phenotype of antibody-mediated rejection in kidney transplant recipients. Kidney Int. 2019;96(1):189–201.

34. Thaunat O, Patey N, Caligiuri G, Gautreau C, Mamani-Matsuda M, Mekki Y, et al. Chronic rejection triggers the development of an aggressive intragraft immune response through recapitulation of lymphoid organogenesis. J Immunol. 2010;185(1):717–28.

35. Kerjaschki D, Regele HM, Moosberger I, Nagy-Bojarski K, Watschinger B, Soleiman A, et al. Lymphatic neoangiogenesis in human kidney transplants is associated with immunologically active lymphocytic infiltrates. J Am Soc Nephrol. 2004;15(3):603–12.

36. Karahan GE, Krop J, Wehmeier C, De Vaal YJH, Langerak-Langerak J, Roelen DL, et al. An easy and sensitive method to profile the antibody specificities of HLA-specific memory b cells. Transplantation. 2019;103(4):716–23.

37. Bradley JA, Mowat AMI, Bolton EM. Processed MHC class I alloantigen as the stimulus for CD4+ T-cell dependent antibody-mediated graft rejection. Immunol Today. 1992;13(11):434–8.

38. Steele DJR, Laufer TM, Smiley ST, Ando Y, Grusby MJ, Glimcher LH, et al. Two levels of help for B cell alloantibody production. J Exp Med. 1996;183(2):699–703.

39. Lúcia M, Luque S, Crespo E, Melilli E, Cruzado JM, Martorell J, et al. Preformed circulating HLA-specific memory B cells predict high risk of humoral rejection in kidney transplantation. Kidney Int. 2015;88(4):874–87.

40. Kohei N, Tanaka T, Tanabe K, Masumori N, Dvorina N, Valujskikh A, et al. Natural killer cells play a critical role in mediating inflammation and graft failure during antibody-mediated rejection of kidney allografts. Kidney Int. 2016;89(6):1293–306.

41. Hidalgo LG, Sis B, Sellares J, Campbell PM, Mengel M, Einecke G, et al. NK cell transcripts and NK cells in kidney biopsies from patients with donor-specific antibodies: Evidence for NK cell involvement in antibody-mediated rejection. Am J Transplant. 2010;10(8):1812–22.

42. Zhang Z, Huang X, Jiang J, Lau A, Yin Z, Liu W, et al. Natural killer cells mediate long-term kidney allograft injury. 2015;99(5).

43. Zhang Z-X, Wang S, Huang X, Min W-P, Sun H, Liu W, et al. NK cells induce apoptosis in tubular epithelial cells and contribute to renal ischemia-reperfusion injury. J Immunol. 2008;181(11):7489–98.

44. Stern M, Elsässer H, Hönger G, Steiger J, Schaub S, Hess C. The number of activating KIR genes inversely correlates with the rate of CMV infection/reactivation in kidney transplant recipients. Am J Transplant. 2008;8(6):1312–7.

45. Lanier LL. Up on the tightrope: Natural killer cell activation and inhibition. Nat Immunol. 2008;9(5):495–502.

46. Costanzo MC, Kim D, Creegan M, Lal KG, Ake JA, Currier JR, et al. Transcriptomic signatures of NK cells suggest impaired responsiveness in HIV-1 infection and increased activity post-vaccination. Nat Commun. 2018;9(1):1212.

47. Wu WK, Famure O, Li Y, Kim SJ. Delayed graft function and the risk of acute rejection in the modern era of kidney transplantation. Kidney Int. 2015;88(4):851–8.

TABLES

Table 1. Demographic and clinical characteristics

	No ABMRh (n=168)	ABMRh (n=56)	P-value	HLA-DSA negative ABMRh (n=26)	HLA-DSA positive ABMRh (n=30)	P-value
Recipient						
Age at transplantation (years), mean (± std)	49.2 (±14.9)	47.6 (±14.6)	0.480	52.5 (±12.7)	43.3 (±15.0)	**0.017**
Gender (female), n (%)	72/172 (42.9)	25/56 (44.6)	0.815	12/26 (46.2)	13/30 (43.3)	0.832
Ethnicity						
Caucasian, n (%)	148/167 (88.6)	48/56 (85.7)	0.826	23/26 (88.5)	25/30 (83.3)	0.801
African, n (%)	6/167 (3.6)	2/56 (3.6)	0.826	1/26 (3.9)	1/30 (3.3)	0.801
Asian, n (%)	4/167 (2.4)	1/56 (1.8)	0.826	0/26 (0.0)	1/30 (3.3)	0.801
Other, n (%)	9/167 (5.4)	5/56 (8.9)	0.826	2/26 (7.7)	3/30 (10.0)	0.801
Repeat transplantation, n (%)	28/168 (16.7)	17/56 (30.4)	**0.027**	6/26 (23.1)	11/30 (36.7)	0.270
Immunological profile						
Anti-HLA DSA ever present, n (%)	54/168 (32.1)	30/56 (53.6)	**0.004**	0/26 (0.0)	30/30 (100.0)	**<0.001**
Anti-HLA DSA at biopsy, n (%)	19/154 (12.3)	18/55 (32.7)	**<0.001**	0/26 (0.0)	18/29 (62.1)	**<0.001**
Anti-HLA DSA at transplantation, n (%)	33/159 (20.8)	19/55 (34.6)	**0.04**	0/26 (0.0)	19/29 (65.5)	**<0.001**
Anti-HLA antibodies ever present, n (%)	87/168 (51.8)	44/56 (78.6)	**<0.001**	14/26 (53.9)	30/30 (100.0)	**<0.001**
Donor						
Age (years), mean (± std)	48.7 (±15.9)	47.6 (±14.4)	0.649	50.8 (±14.8)	44.7 (±13.6)	0.122
Gender (female), n (%)	76/156 (48.7)	30/53 (56.6)	0.321	12/25 (48.0)	18/28 (64.3)	0.233
Living donation, n (%)	33/168 (19.6)	8/55 (14.6)	0.681	3/26 (11.5)	5/29 (17.2)	0.727
Donation after brain death, n (%)	119/168 (70.8)	42/55 (76.4)	0.306	20/26 (76.9)	22/29 (75.9)	0.727
Donation after circulatory death, n (%)	16/168 (9.5)	5/55 (9.1)	0.306	3/26 (11.5)	2/29 (6.9)	0.727
Biopsy						
Days post transplantation, median (IQR)	370 (93-928)	361 (40-1059)	0.246	250 (16-708)	361 (84-1777)	0.304
Context						

Indication, n(%)	49/168 (29.2)	36/56 (64.3)	**<0.001**	18/26 (69.2)	18/30 (60.0)	0.472
Protocol, n(%)	119/168 (70.8)	20/56 (35.7)	**<0.001**	8/26 (30.8)	12/30 (40.0)	0.472
eGFR (ml/min/1,73m²), mean (± std)	45.1 (±20.3)	30.6 (±20.3)	**<0.001**	25.8 (± 16.6)	34.8 (± 21.7)	0.092
Proteinuria (g/g creatinine), median (IQR)	0.13 (0.07-0.25)	0.46 (0.19-1.78)	**<0.001**	0.39 (0.15-1.36)	0.78 (0.3-2.26)	0.189
Immunosuppression						
Cyclosporin, n (%)	11/168 (6.6)	7/56 (12.5)	0.156	4/26 (15.4)	3/30 (10.0)	0.693
Tacrolimus, n (%)	147/168 (87.5)	46/56 (82.1)	0.315	20/26 (76.9)	26/30 (86.7)	0.487
Mycophenolate mofetil, n(%)	155/168 (92.3)	49/56 (87.5)	0.279	23/26 (88.5)	26/30 (86.7)	1.000
Azathioprine, n(%)	7/168 (4.2)	0/56 (0.0)	0.197	0/24 (0.0)	0/28 (0.0)	1.000
mTOR inhibitor, n(%)	8/168 (4.8)	6/56 (10.7)	0.111	3/26 (11.5)	3/30 (10.0)	1.000
Corticosteroids, n (%)	141/168 (83.9)	52/56 (92.9)	0.094	24/26 (92.3)	28/30 (93.3)	1.000
Treatment after ABMRh diagnosis, n(%)	-	-	-	18/26 (69.2%)	18/30 (60.0%)	0.472
Corticosteroids, n(%)	-	-	-	17/18 (94.4%)	16/18 (88.9%)	1.000
Anti-thymocyte globulin, n(%)	-	-	-	3/18 (16.7%)	2/18 (11.1%)	1.000
Intravenous immunoglobulin, n(%)	-	-	-	2/18 (11.1%)	8/18 (44.4%)	**0.026**
Plasmapheresis, n(%)	-	-	-	4/18 (22.2%)	9/18 (50.0%)	0.083
Rituximab, n(%)	-	-	-	2/18 (11.1%)	5/18 (27.8%)	0.207
Eculizumab, n(%)	-	-	-	0/18 (0.0%)	1/18 (5.6%)	1.000
Transplantation						
Delayed graft function, n (%)	29/167 (17.4)	19/55 (34.6)	**0.007**	12/26 (46.2)	7/29 (24.1)	0.087
Cold ischemia time (hours), median (IQR)	12.6 (7.9-16.9)	13.0 (7.9-17.7)	0.513	11.9 (7.9-16.2)	15.3 (7.0-17.8)	0.303
Warm ischemia time (hours), median (IQR)	0.3 (0.1-0.4)	0.3 (0.1-0.4)	0.765	0.4 (0.1-0.4)	0.1 (0.1-0.2)	0.773
Immunosuppression						
Induction therapy, n (%)	116/167 (69.5)	44/54 (81.5)	0.086	21/26 (80.8)	23/28 (82.1)	1.000
ATG, n (%)	15/116 (12.9)	7/44 (15.9)	0.878	3/21 (14.3)	4/23 (17.4)	1.000
Anti-CD25, n (%)	98/116 (84.5)	36/44 (81.8)	0.878	18/21 (85.7)	18/23 (78.3)	1.000
Other, n(%)	2/116 (1.72)	1/44 (2.3)	0.878	0/21 (0.0)	1/23 (4.4)	1.000
Cyclosporin, n (%)	27/168 (16.1)	10/56 (17.9)	0.755	4/26 (15.4)	6/30 (20.0)	0.737
Tacrolimus, n (%)	139/168 (82.7)	46/56 (82.1)	0.919	22/26 (84.6)	24/30 (80.0)	0.737
Mycophenolate mofetil, n(%)	156/168 (92.9)	51/56 (91.1)	0.662	24/26 (92.3)	27/30 (90.0)	1.000

Azathioprine, n(%)	2/168 (1.2)	0/56 (0.0)	1.000	0/24 (0.0)	0/28 (0.0)	1.000
mTOR inhibitor, n(%)	4/168 (2.4)	3/56 (5.4)	0.371	1/26 (4.2)	2/30 (6.7)	1.000
Corticosteroids, n (%)	167/168 (99.4)	56/56 (100.0)	1.000	26/26 (100)	30/30 (100.0)	1.000

Denominator numbers less than original group size indicate incomplete information. Percentage values may not add up to 100% due to rounding. Bold numbers indicate significant P-values for difference between groups. ABMRh: histology of antibody-mediated rejection, DSAposBMRh: DSA positive ABMRh, DSAnegABMRh: DSA negative ABMRh, IQR: inter-quartile range, DSA: donor-specific antibodies, eGFR: estimated glomerular filtration rate, ATG: anti-thymocyte globulin, mTOR: mammalian target of rapamycin.

Table 2 Comparison of histological features between phenotypes

Parameter	No ABMRh (n=168)	ABMRh (n=56)	P-value	HLA-DSA negative ABMRh (n=26)	HLA-DSA positive ABMRh (n=30)	P-value
g, mean (±std)	0.05 (±0.22)	1.95 (±0.94)	**<0.001**	2.19 (±0.80)	1.73 (±1.01)	0.089
g≥1, n(%)	9/168 (5.4)	53/56 (94.6)	**<0.001**	26/26 (100.0)	27/30 (90.0)	0.240
ptc, mean (±std)	0.09 (±0.43)	1.07 (±0.89)	**<0.001**	1.12 (±0.82)	1.03 (±0.96)	0.659
ptc≥1, n(%)	9/168 (5.4)	39/56 (69.6)	**<0.001**	20/26 (76.9)	19/30 (63.3)	0.270
mvi score, mean (±std)	0.14 (±0.47)	3.01 (±1.30)	**<0.001**	3.31 (±1.09)	2.77 (±1.43)	0.128
mvi ≥2, n(%)	4/168 (2.4)	49/56 (87.5)	**<0.001**	25/26 (96.2)	24/30 (80.0)	0.108
C4d, mean (±std)	0.12 (±0.55)	0.84 (±1.16)	**<0.001**	0.46 (±0.81)	1.17 (±1.32)	**0.040**
C4d≥1, n(%)	9/168 (5.4)	24/56 (42.9)	**<0.001**	8/26 (30.8)	16/30 (53.3)	0.089
v, mean (±std)	0.04 (±0.22)	0.38 (±0.65)	**<0.001**	0.42 (±0.58)	0.33 (±0.71)	0.293
v≥1, n(%)	5/168 (3.0)	17/56 (30.4)	**<0.001**	10/26 (38.5)	7/30 (23.3)	0.220
cg, mean (±std)	0.07 (±0.41)	0.40 (±0.81)	**<0.001**	0.35 (±0.63)	0.45 (±0.95)	0.938
cg≥1, n(%)	7/168 (4.2)	14/56 (25.0)	**<0.001**	7/26 (26.9)	7/30 (23.3)	0.768
i, mean (±std)	0.24 (±0.65)	0.63 (±1.05)	**0.006**	0.77 (±1.21)	0.50 (±0.90)	0.424
i≥1, n(%)	25/168 (14.9)	17/56 (30.4)	**0.010**	9/26 (34.6)	8/30 (26.7)	0.519
t, mean (±std)	0.44 (±0.76)	0.70 (±0.76)	**0.004**	0.69 (±0.88)	0.70 (±0.65)	0.654
t≥1, n(%)	52/168 (31.0)	30/56 (53.6)	**0.003**	12/26 (46.2)	18/30 (60.0)	0.300
ti, mean (±std)	0.38 (±0.79)	0.57 (±0.87)	**0.040**	0.46 (±0.86)	0.67 (±0.88)	0.299
ti≥1, n(%)	38/168 (22.6)	21/56 (37.5)	**0.029**	8/26 (30.8)	13/30 (43.3)	0.333

ci, mean (±std)	0.94 (±1.10)	0.68 (±0.79)	0.288	0.54 (±0.71)	0.80 (±0.85)	0.246
ci≥1, n(%)	87/168 (51.8)	24/56 (42.8)	0.576	11/26 (42.3)	17/30 (56.7)	0.284
ct, mean (±std)	1.01 (±1.01)	0.80 (±0.72)	0.401	0.73 (±0.67)	0.87 (±0.78)	0.578
ct≥1, n(%)	103/168 (61.3)	36/56 (64.3)	0.691	16/26 (61.5)	20/30 (66.7)	0.690
ah, mean (±std)	0.85 (±0.99)	1.04 (±1.11)	0.324	1.08 (±1.06)	1.00 (±1.17)	0.609
ah≥1, n(%)	88/168 (52.4)	32/56 (57.1)	0.536	17/26 (65.4)	15/30 (50.0.4)	0.246
cv, mean (±std)	0.83 (±0.95)	1.20 (±1.15)	**0.043**	1.42 (±1.21)	1.00 (±1.08)	0.187
cv≥1, n(%)	87/168 (51.8)	35/56 (62.5)	0.163	18/26 (70.8)	17/30 (56.7)	0.333
TCMR, n(%)	10/168 (6.0)	14/56 (25.0)	**<0.001**	8/26 (30.8)	6/30 (20.0)	0.353
Borderline, n(%)	20/168 (11.9)	6/56 (10.7)	0.810	2/26 (7.7)	4/30 (13.3)	0.675
IFTA, n(%)	80/168 (47.6)	24/56 (42.9)	0.536	11/26 (42.3)	13/30 (43.3)	0.938
PVAN, n(%)	2/168 (1.2)	1/56 (1.8)	1.000	0/26 (0.0)	1/30 (3.3)	1.000
ATN, n(%)	34/168 (20.2)	22/56 (39.3)	**0.004**	9/26 (34.6)	13/30 (43.3)	0.505
GNF, n(%)	1/168 (0.6)	3/56 (5.4)	**0.049**	2/26 (7.7)	1/30 (3.3)	0.592
TMA, n(%)	3/168 (1.8)	6/56 (10.7)	**0.009**	3/26 (11.5)	3/30 (10.0)	1.000
Pyelonephritis, n(%)	3/168 (1.8)	0/56 (0.0)	0.574	0/24 (0.0)	0/30 (0.0)	1.000

Denominator numbers less than original group size indicate missing data. Percentage values may not add up to 100% due to rounding. Bold numbers indicate significant P-values for difference between groups. TCMR: T cell-mediated rejection, IFTA: interstitial fibrosis and tubular atrophy, PVAN: polyoma virus-associated nephropathy, ATN: acute tubular necrosis, GNF: glomerulonephritis, TMA: thrombotic microangiopathy.

Table 3 Cox proportional hazards analysis of allograft failure (N=224)

Factor	No. of patients	No. of events	Univariate analysis			Multivariate analysis		
			HR	**95% CI**	**P-value**	**HR**	**95% CI**	**P-value**
HLA-DSA ABMRh								
No ABMRh	168	16	1			1		
HLA-DSA negative ABMRh	26	6	2.57	1.00-6.58	**0.049**	2.33	0.85-6.33	0.099
HLA-DSA positive ABMRh	30	12	5.39	2.55-11.43	**<0.001**	7.24	3.04-17.20	**<0.001**
C4d score	224	34	1.08	0.74-1.57	0.689	0.68	0.43-1.06	0.091
Cellular rejection								
None	174	21	1			1		
Borderline	26	5	1.72	0.65-4.56	0.277	1.76	0.66-4.68	0.260
TCMR	24	8	3.27	1.45-7.39	**0.004**	2.09	0.88-4.99	0.097

Bold numbers indicate significant P-values. ABMRh: histology of antibody-mediated rejection, HLA-DSA: anti-HLA donor specific antibodies, TCMR: T cell-mediated rejection. HR: hazard ratio.

FIGURE LEGENDS

Figure 1. Transcriptional similarity between HLA-DSA positive and HLA-DSA negative ABMRh

(A) Differential gene expression analysis between ABMRh (n=56) and No ABMRh (n=168). Genes can be represented by multiple probesets within a single microarray. FDR-adjusted P-value <0.01 was considered significant (dashed red line).

(B) Differential gene expression analysis between HLA-DSA negative ABMRh (n=26) and HLA-DSA positive ABMRh (n=30). No probesets were found to differ between these two groups after FDR-adjustment, despite a clear distinction between ABMRh cases and other biopsies as presented in panel A.

(C) Ingenuity pathway analysis of differentially expressed genes in ABMRh, HLA-DSA positive ABMRh or HLA-DSA negative ABMRh vs. other biopsies. The top 10 upregulated pathways in ABMRh were preserved in both ABMRh subtypes. Gene proportion denotes the fraction of known genes within the analysed pathway that are significantly overexpressed.

FIGURE 1

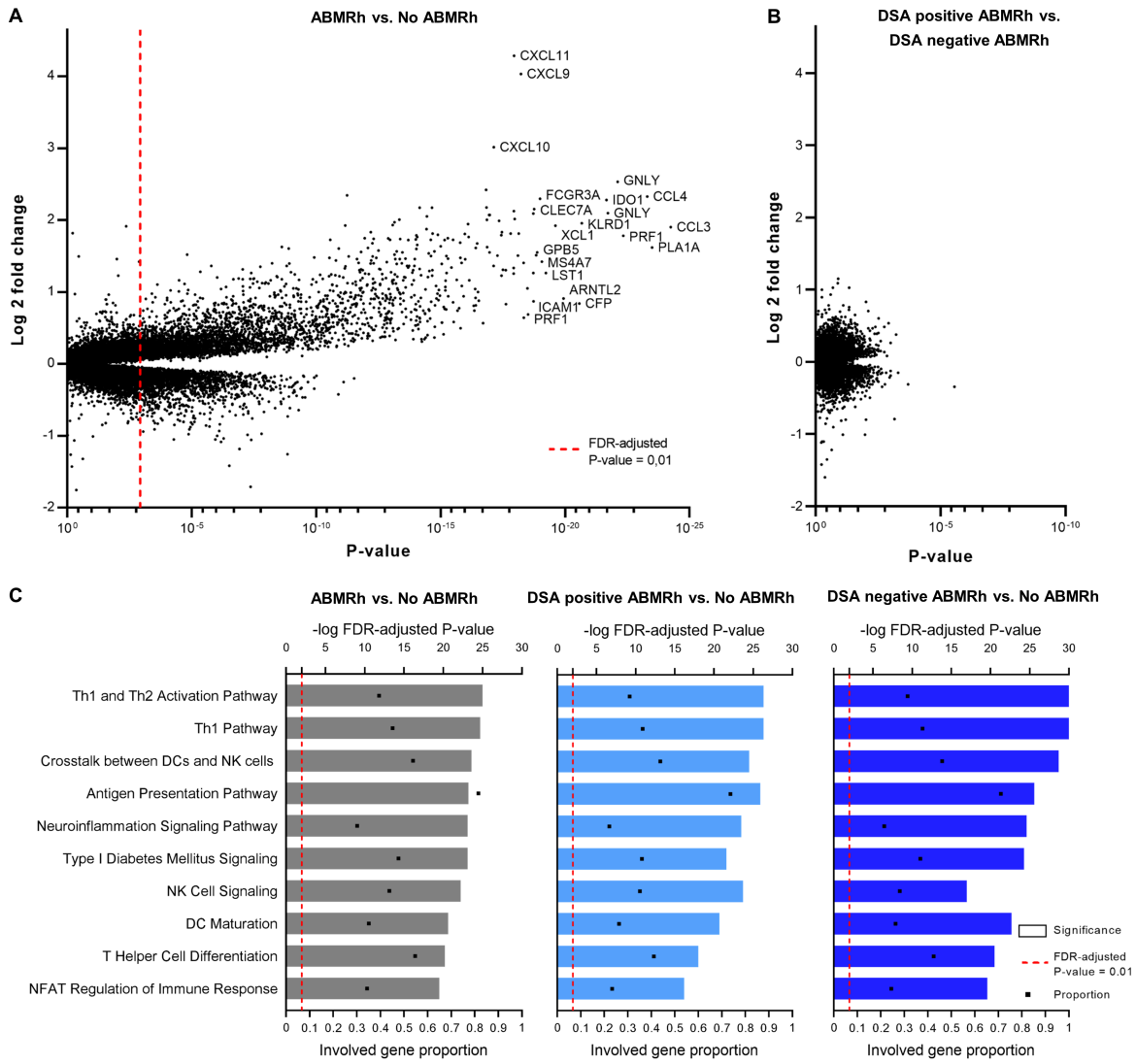
A
ABMRh vs. No ABMRh
Log 2 fold change
P-value
CXCL11
CXCL9
CXCL10
GNLY
FCGR3A
IDO1
CCL4
CLEC7A
GNLY
KLRD1
CCL3
XCL1
PRF1
PLA1A
GPB5
MS4A7
LST1
ARNTL2
ICAM1
CFP
PRF1
FDR-adjusted
P-value = 0,01
B
DSA positive ABMRh vs.
DSA negative ABMRh
Log 2 fold change
P-value
C
ABMRh vs. No ABMRh
DSA positive ABMRh vs. No ABMRh
DSA negative ABMRh vs. No ABMRh
-log FDR-adjusted P-value
Th1 and Th2 Activation Pathway
Th1 Pathway
Crosstalk between DCs and NK cells
Antigen Presentation Pathway
Neuroinflammation Signaling Pathway
Type I Diabetes Mellitus Signaling
NK Cell Signaling
DC Maturation
T Helper Cell Differentiation
NFAT Regulation of Immune Response
Involved gene proportion
Significance
FDR-adjusted
P-value = 0.01
Proportion

Figure 2. Leukocyte infiltration and ABMR histology

(A) Heatmap of Spearman correlation coefficients between absolute leukocyte infiltration and severity of histological lesions in HLA-DSA negative (n=140) and HLA-DSA positive patients (n=84). Marked boxes indicate statistical significance ($P < 0.05$).

(B-C) ROC curves depicting diagnostic accuracy of lymphoid (B) and myeloid (C) cell infiltration for and between ABMRh subtypes. Infiltration of NK cells, monocytes/macrophages and CD8 positive T cells had the highest predictive value for ABMRh, regardless of HLA-DSA status.

The heatmap for the entire population and ROC curves for ABMRh are depicted in Figure S2.

FIGURE 2

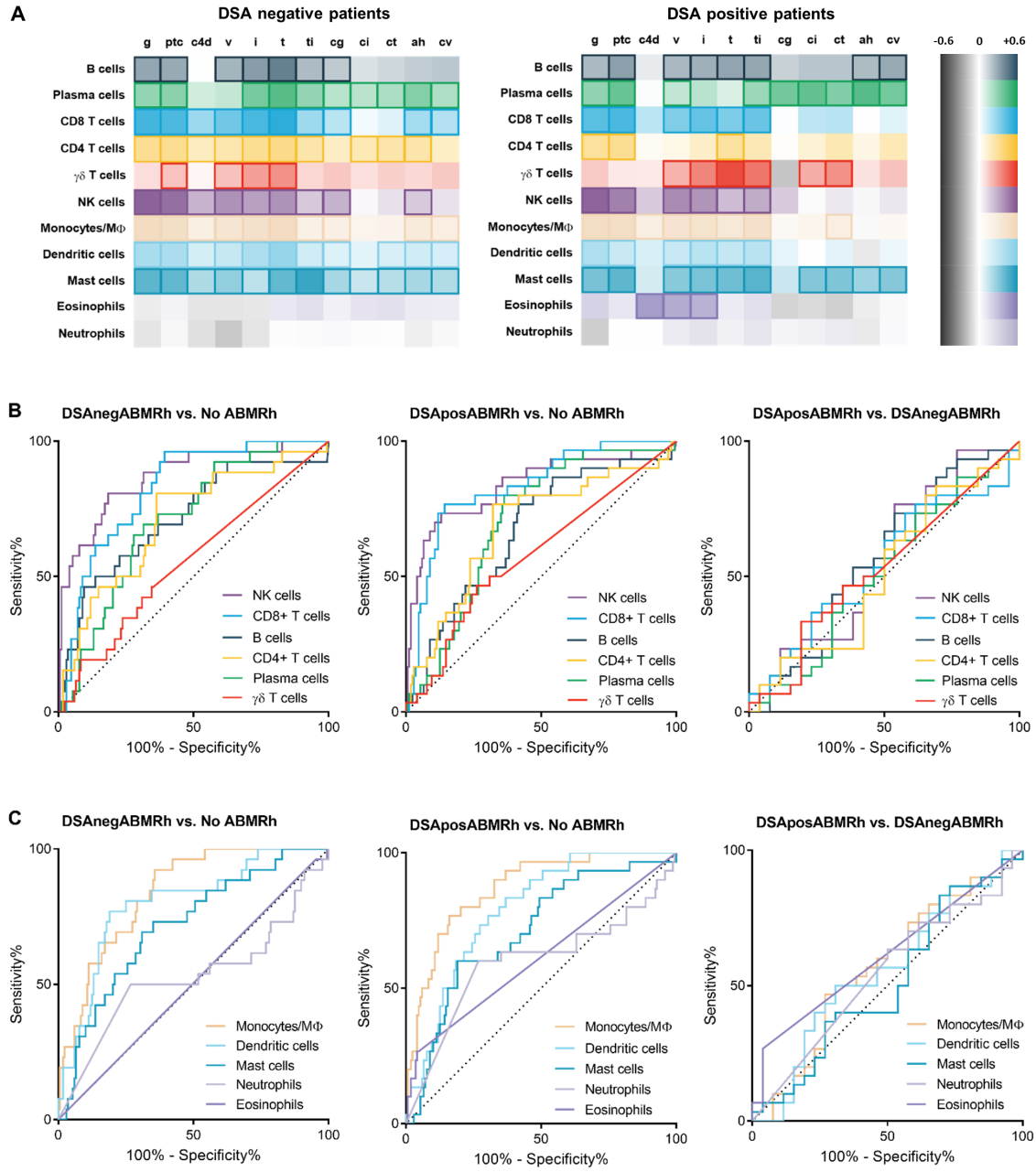
A
DSA negative patients
DSA positive patients
g ptc c4d v i t ti cg ci ct ah cv
-0.6 0 +0.6
B cells
Plasma cells
CD8 T cells
CD4 T cells
γδ T cells
NK cells
Monocytes/MΦ
Dendritic cells
Mast cells
Eosinophils
Neutrophils
B
DSAnegABMRh vs. No ABMRh
DSAposABMRh vs. No ABMRh
DSAposABMRh vs. DSAnegABMRh
Sensitivity%
100% - Specificity%
NK cells
CD8+ T cells
B cells
CD4+ T cells
Plasma cells
γδ T cells
C
DSAnegABMRh vs. No ABMRh
DSAposABMRh vs. No ABMRh
DSAposABMRh vs. DSAnegABMRh
Sensitivity%
100% - Specificity%
Monocytes/MΦ
Dendritic cells
Mast cells
Neutrophils
Eosinophils

Figure 3. Leukocyte subset infiltration in microvascular inflammation

Principal component analysis of leukocyte subset infiltration quantified by computer-assisted analysis of immunohistochemical staining in kidney allografts with microvascular inflammation (MVI), in the presence (n=32) or absence (n=15) of circulating HLA-DSA. Plotted 95% confidence ellipses show major areas of overlap.

FIGURE 3

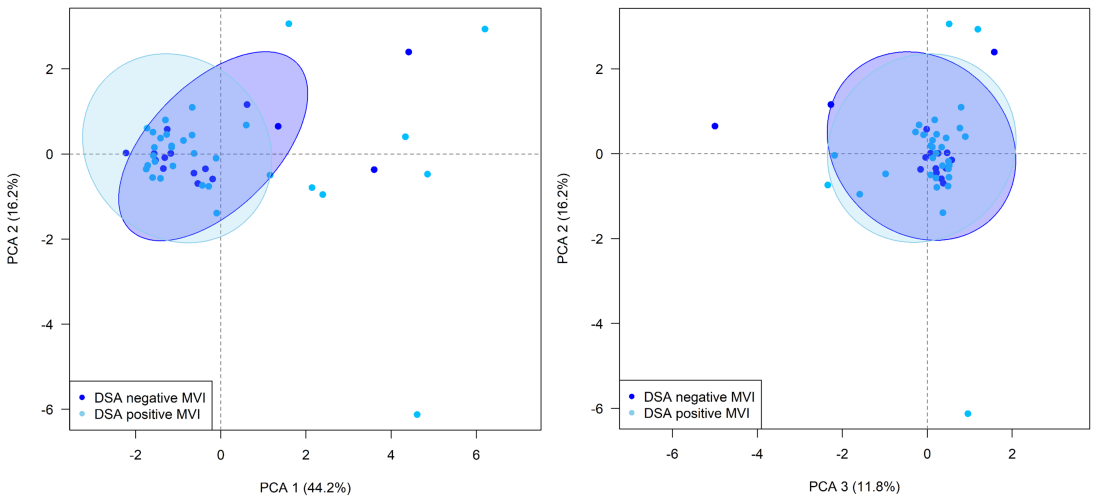

Figure 4. **Molecular heterogeneity of ABMRh biopsies**

(A-D) Clustering of all allograft biopsies (N=224) based on expression of all genes (A) and gene subsets (B-D) distinguished most ABMRh biopsies. Ten ABMRh cases were persistent outliers.

(E-H) Among ABMRh biopsies (n=56), transcriptional heterogeneity was not explained by HLA-DSA or C4d severity, whereas biopsies with mixed rejection (concomitant borderline/TCMR) colocalize.

t-SNE was used for dimensionality reduction. Points represent individual biopsies

FIGURE 4

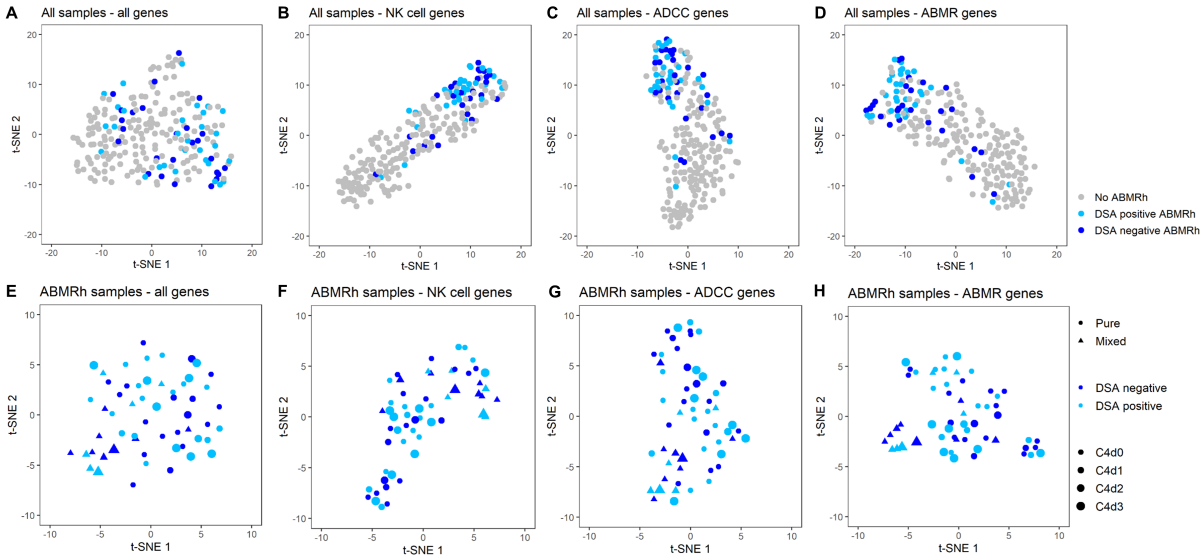

.

Figure 5. ABMR lesion severity and gene expression

Clustering of biopsies based on expression of selective gene sets, with labelling based on the histomorphological humoral lesion score (i.e. sum of g, ptc, v, C4d and cg lesions). In both HLA-DSA positive (n=84) and HLA-DSA negative patients (n=140), ADCC, NK cell and ABMR transcripts associate with severity of humoral scores. t-SNE is used for dimensionality reduction. Points represent biopsies.

FIGURE 5

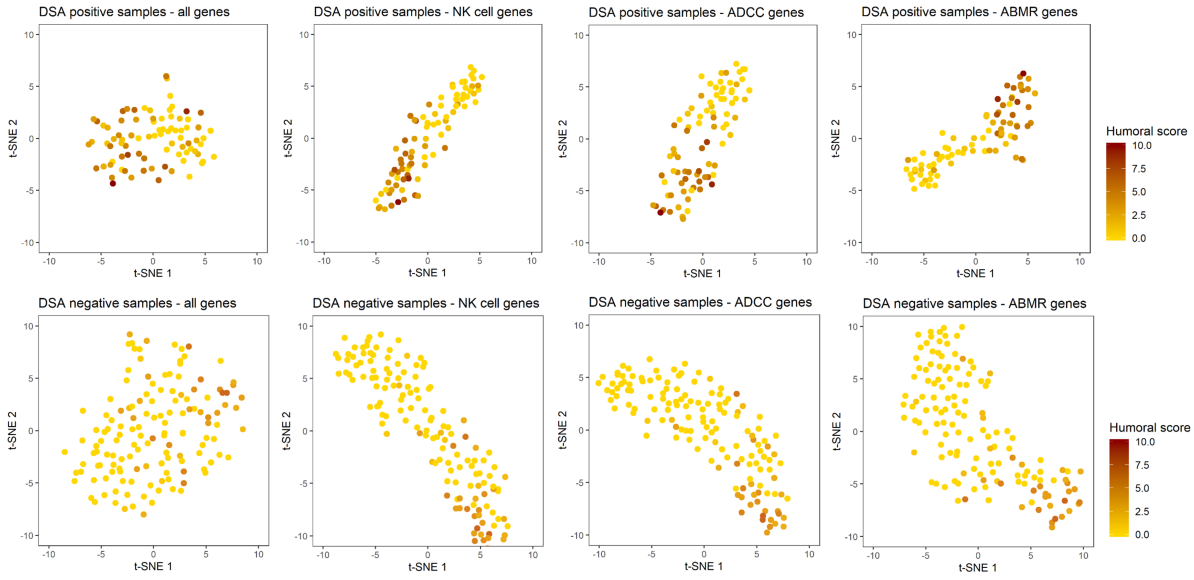

Figure 6. Module-trait relationships in a weighted gene co-expression network analysis (WGCNA) in ABMRh biopsies (n=56)

Heatmap represents the correlation between the 37 detected modules (Y-axis) and different traits of interest (X-axis). Color represent log 10 P-values after FDR-adjustment, numbers represent strength of the association (biweight midcorrelation coefficient). HLA-DSA status, C4d score and borderline rejection did not significantly correlate with modules within ABMRh, in contrast to TCMR.

FIGURE 6

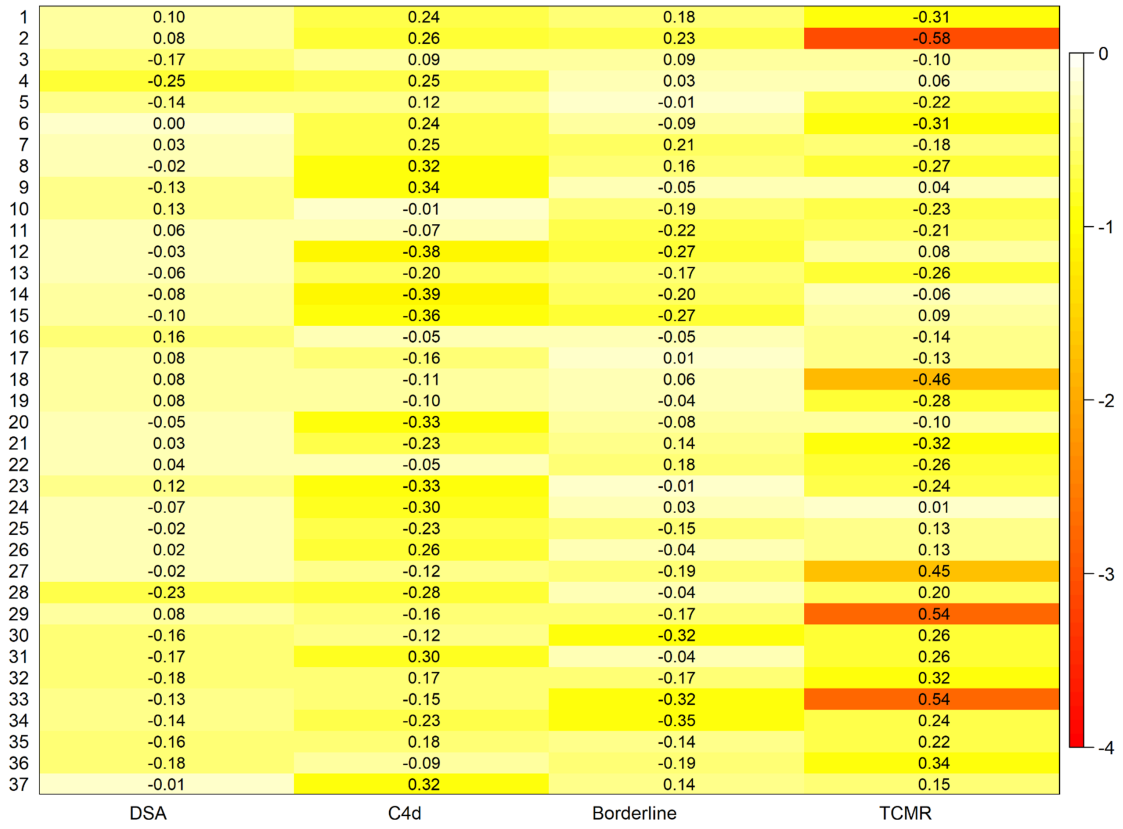

Figure 7. HLA-DSA status, ABMR histology and graft failure

(A-C) Kaplan-Meier curves of death-censored allograft survival based on ABMR histology with HLA-DSA, C4d positivity or cellular rejection. C4d positivity is defined as a C4d score > 0 by immunohistochemistry, or C4d > 1 by immunofluorescence. Cellular rejection denotes borderline or TCMR.

(D-F) Survival analysis based on average expression of selected gene sets, and HLA-DSA. High molecular scores were defined as above the median value in the entire cohort.

FIGURE 7